Layered Compounds

Deutsche Ausgabe: DOI: 10.1002/ange.201509953
Internationale Ausgabe: DOI: 10.1002/anie.201509953

Efficient MoS_2 Exfoliation by Cross-β-Amyloid Nanotubes for Multistimuli-Responsive and Biodegradable Aqueous Dispersions

*Nidhi Kapil, Ashmeet Singh, Manish Singh, and Dibyendu Das**

Abstract: *Herein, we report the efficient exfoliation of MoS_2 in aqueous medium by short cationic peptide nanotubes featuring the nucleating core ^{17}LVFFA^{21} of β-amyloid (Aβ 1–42), a sequence associated with Alzheimer's disease. The role of morphology, length, and nature of the amyloid surface on exfoliation/dispersions of MoS_2 were investigated through specific mutations of the amyloid sequences. Notably, owing to the properties of both the constituents, self-assembled soft nanostructures and MoS_2, the hybrid dispersions responded reversibly to various stimuli, including temperature, pH, and light. Addition of a protease resulted in loss of the dispersions, which are otherwise stable for months at ambient conditions. The design flexibility of the peptide sequences, along with the stimuli-responsiveness and biodegradability, can complement the applications of MoS_2 in diverse fields.*

Molybdenum disulfide (MoS_2), belonging to the family of layered transition metal dichalcogenides (TMDs), have garnered immense attention in recent years, particularly after the great advancements witnessed in the applications of graphene.[1] Exceptional layer-dependent properties of MoS_2 are observed when the size of the TMDs decrease from three dimensions to two dimensions.[1a–d,2] Applications of these thin layers of MoS_2 have been realized in diverse fields, such as catalysis, solid lubrication, energy storage, photovoltaics, and thermoelectric materials.[1a–d,2,3] The unique optical properties and large surface area of thin layers of MoS_2 have recently been exploited in elegant biomedicinal works.[4] However, strong interlayer van der Waals interactions result in very poor solubility of these layered materials.[5] Also, the high surface energy of MoS_2 in the range of 250 mJ m^{-2} limits the use of environmentally friendly aqueous media.[5a] Many recent works have used reagents, such as oleum, H_2O_2, and ionic liquids, for assisting the exfoliation of MoS_2 in aqueous solvent.[4a,d,6] On the other hand, Coleman et al. have extensively used commercial surfactants for large-scale aqueous exfoliation of layered materials where colloidal stability is achieved from the charge repulsion of the surfactant coating.[5a] Interestingly, intercalation of cationic species, such as lithium ions and even organic polycations based on pyrrole and aniline, have been used to inhibit the reaggregation of exfoliated MoS_2 layers.[2c,4e,7] However, these procedures are time consuming, require harsh conditions, involve toxic reagents, and are sensitive to the environment. Therefore, it would be intriguing to find exfoliating agents for MoS_2 in aqueous medium that are purely derived from natural precursors and that are environmentally benign.

In this context, highly cationic surfaces of cross-β-amyloid nanostructures have been shown to bind diverse molecular architectures and surfaces, along with the capability to impart colloidal stability.[1e,8] Additionally, these short peptide-based nanostructures can be designed to be acutely responsive to different physical and chemical environmental inputs.[9] In an attempt to find an environmentally benign way of making MoS_2 dispersions which can be biodegradable and respond reversibly to external inputs, amyloid nanostructures created from ^{17}LVFFA^{21} of βamyloid (Aβ 1–42; Figure 1) were used to exfoliate MoS_2 in water.

To check the capability of amyloid nanostructures for MoS_2 exfoliation, we started with Ac-KLVFFAE-NH_2 from 16–22 residues of wildtype Aβ.[8a,9c] Ac-KLVFFAE-NH_2 assembles to form classical amyloid fibrils with lengths of several microns and diameters of approximately 15 nm (Supporting Information, Figure S1). Briefly, powdered MoS_2 (6 mg) was added to an aqueous dispersion of Ac-KLVFFAE-NH_2 (3.5 mM, 2 mL) and sonicated (tip) for 30 min (Supporting Information). The resulting aqueous greenish black dispersion of MoS_2 remained stable for weeks (Figure 1C). The UV/Vis-NIR spectrum showed characteristic peaks at 448, 451, 610, and 672 nm, indicating efficient MoS_2 exfoliation (Figure 2B).[1d,5b,10] As previously reported, the amount of dispersed MoS_2 was calculated by the filtration and weighing method (Supporting Information).[4a,5a,6] The amount of dispersed MoS_2 was found to be 0.09 mg mL^{-1} (Figure 2A; Supporting Information, Table S1). To investigate the role of amyloid morphology on exfoliation, Ac-KLVFFAE-NH_2 was assembled at pH 2 (Supporting Information).

At pH 2, Ac-KLVFFAE-NH_2 formed nanotubes with diameters of 35–40 nm[9c] and lengths up to 10 microns (Figure 1D). Nanotube morphology was found to be better for MoS_2 exfoliation as the amount of dispersed MoS_2 increased to 0.16 mg mL^{-1}. To remove the effect of pH, a glutamic acid residue was changed to leucine to form Ac-KLVFFAL-NH_2, which at neutral pH assembled to form homogenous nanotubes with diameters of 35–40 nm (Figure 1E).[8a,b] The amount of dispersed MoS_2 increased further with Ac-KLVFFAL-NH_2 nanotubes to 0.18 mg mL^{-1}. Under

[*] N. Kapil, A. Singh, Dr. M. Singh
Institute of Nano Science and Technology, Phase 10
Mohali 160062 (India)
Dr. D. Das
Indian Institute of Science Education and Research (IISER) Tirupati
Andhra Pradesh 517507 (India)
E-mail: dasd@iisertirupati.ac.in
ddas.chem@gmail.com

Supporting information and the ORCID identification number(s) for the author(s) of this article can be found under http://dx.doi.org/10.1002/anie.201509953.

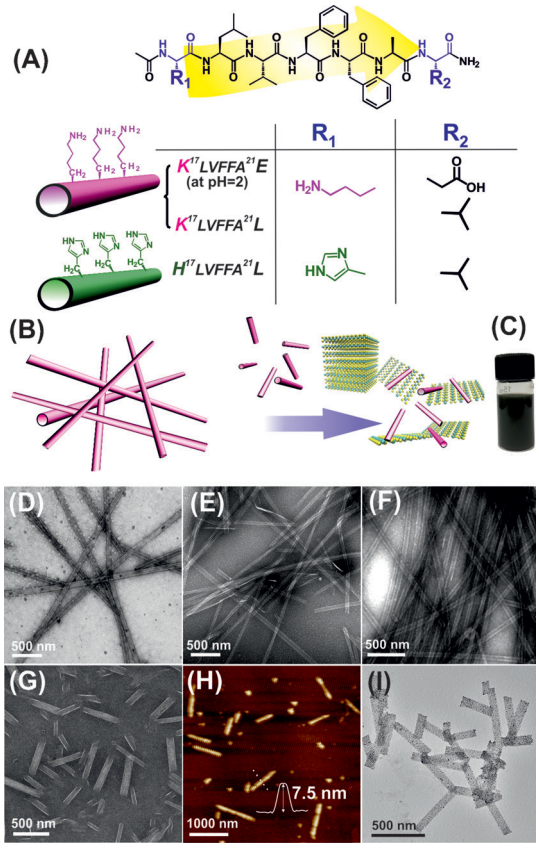

Figure 1. A) Structure of amyloid peptides. B) Representation of MoS_2 exfoliation by cationic amyloid nanotubes. C) Vial showing dispersion of MoS_2 by amyloid nanotubes. D–G) TEM images of nanotubes of D) Ac-KLVFFAE-NH_2 at pH 2, E) Ac-KLVFFAL-NH_2, F) Ac-HLVFFAL-NH_2, G) short Ac-KLVFFAL-NH_2 tubes formed after tip sonication (30 min). H) AFM image of short nanotubes of Ac-KLVFFAL-NH_2 with height profile. I) Anionic gold nanoparticles bound to short tubes without stain.

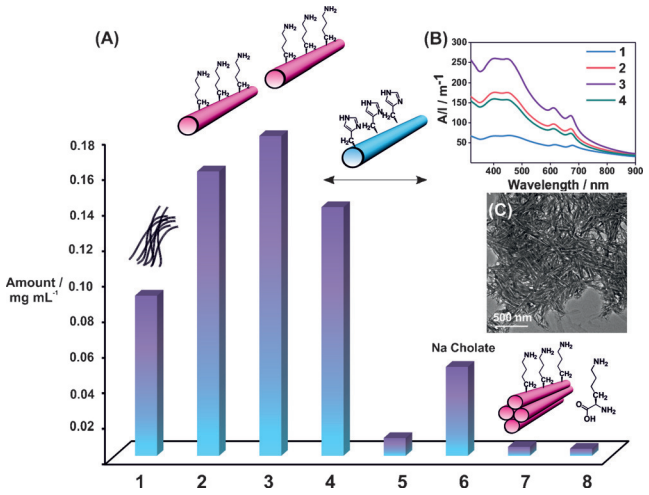

Figure 2. A) Amount of dispersed MoS_2 by Ac-KLVFFAE-NH_2 nanofibers (**1**) Ac-KLVFFAE-NH_2 nanotubes at pH 2 (**2**), Ac-KLVFFAL-NH_2 nanotubes (**3**), Ac-HLVFFAL-NH_2 nanotubes at pH 6.5 (**4**) and at pH 9 (**5**), sodium cholate (**6**), bundled Ac-KLVFFAL-NH_2 nanotubes (**7**), and lysine (**8**). B) Typical UV/Vis absorption spectra of exfoliated MoS_2 in Ac-KLVFFAE-NH_2 nanofibers (**1**), Ac-KLVFFAE-NH_2 nanotubes (**2**), Ac-KLVFFAL-NH_2 nanotubes (**3**), Ac-HLVFFAL-NH_2 nanotubes at pH 6.5 (**4**). C) TEM image of bundled short nanotubes treated with Na_2SO_4. Error ranged from 5–15% in triplicates.

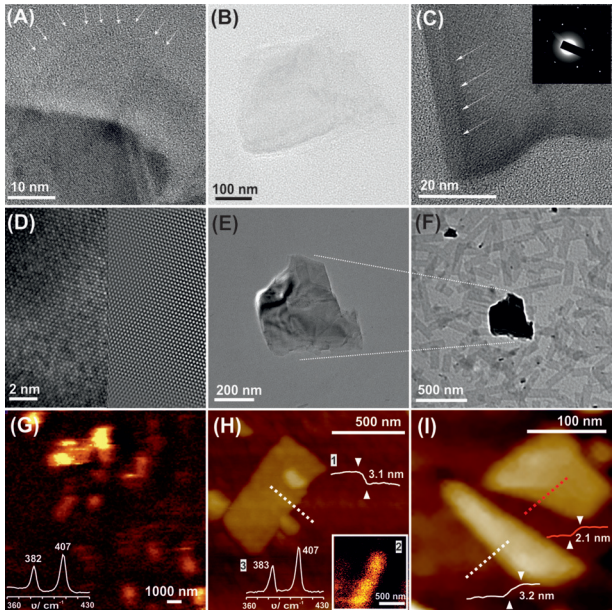

Figure 3. A–C) Bright field TEM images of MoS_2 showing thin layers of MoS_2. C) Zoomed image of MoS_2 indicating 2 layers. Inset in C shows typical electron diffraction pattern. D) Phase contrast and digitally filtered HRTEM of thin layer MoS_2 sheet. E) Thin layer MoS_2 sheet and F) nanotube morphology in the background. G) Raman mapping of MoS_2 deposited on silicon substrate. Inset showing typical Raman spectrum of exfoliated MoS_2. H) AFM image of MoS_2 sheet with insets 1) height profile of the sheet, 2) Raman map and 3) Raman spectra of the same region. I) AFM image of MoS_2 sheets with line profiles given in red and white.

identical conditions, commercial surfactants like sodium cholate and sodium dodecyl benzene sulfonate (SDBS) could only disperse 0.05 and 0.04 mg mL^{-1}, respectively (Figure 2A; Supporting Information, Table S1).

The exfoliated MoS_2 were characterized by TEM, which showed numerous thin flakes (Figure 3A–C), indicating the presence of layers of MoS_2 nanosheets (Figure 3B,C and HRTEM Figure 3D). The lateral sizes of the flakes displayed a wide distribution from 65 nm to 1150 nm, with mean $\langle L \rangle =$ 328 nm (Figure S2C–2H, S3A TEM of precursor MoS_2 powder in Figure S2A,B). The diffraction pattern (Figure 3C inset) suggested an undistorted lattice with hexagonal symmetry.[5a] In an attempt to visualize the nanotubes in the same TEM image frame, which was showing MoS_2 (Figure 3E), the defocus values were changed during imaging. Nanotube morphology could be clearly seen in the background (Figure 3E,F). Interestingly, the lengths of the nanotubes in the background were substantially shorter than the usual length. Consequently, we were curious about the state of the nanotubes after probe sonication. To this end, an aqueous solution of Ac-KLVFFAL-NH_2 (3.5 mM) nanotubes was separately sonicated (tip) for 30 and 60 min. Numerous short fragments of average length 400–550 nm were observed under TEM (Figure 1G; Supporting Information, Figure S4). Atomic force microscopy (AFM) also showed shorter nanotubes (Figure 1H). To confirm that the surface of the short nano-

tubes is cationic, negatively charged citrate-coated gold nanoparticles (−AuNP) were added. TEM showed −AuNP specifically decorated the surfaces, strongly suggesting the presence of a cationic surface. Controls with positively charged gold nanoparticles (+AuNP) did not result in specific binding (Figure S5). At this point, we were curious to investigate whether the shorter length of amyloid nanotubes was playing a role in the efficient exfoliation. For this purpose, exfoliation was attempted with only mechanical stirring conditions and without any sonication (Figure S6). It is important to note here that strong interlayer forces present in MoS_2 necessitate large mechanical forces to overcome and hence sonication (tip) is used for prolonged time intervals.[4,5] Interestingly, the short amyloid tubes were able to disperse MoS_2 even without probe sonication as, after centrifugation, a greenish supernatant was obtained and the UV/Vis spectra showed the characteristic peaks (Figure S6). The longer native tubes were less efficient at exfoliating MoS_2 (Figure S6, S7). Therefore, this experiment reinforced the importance of peptide nanotubes of shorter lengths which provided improved intercalation and colloidal stability to the exfoliated MoS_2.

To confirm the thin layers (Figure 3 A–D, Figure S2) were indeed MoS_2, Raman mapping of the samples (Figure 3 G) was done. Intense peaks at 382 and 407 cm^{-1} (inset of Figure 3 G) were observed, confirming the presence of undistorted structure of 2H MoS_2, a finding also supported from the diffraction pattern.[5a,11] In contrast, harsh methods of ion intercalation often result in generation of distorted 2H structure of bulk MoS_2.[5a] The layer thicknesses were monitored by AFM. However, samples prepared directly from MoS_2-Ac-KLVFFA**L**-NH_2 solutions showed densely populated short nanotubes (Figure S8). To image the sheets, the dispersions were diluted with water, before drop casting on silicon surface (Supporting Information). AFM showed numerous thin flakes (Figure 3 H–I; Supporting Information, Figure S2 I–L) which were confirmed to be MoS_2 from Raman Spectroscopy (Figure 3 H, inset). The height analyses showed a distribution with highest populations in the range from 2–3.5 nm, which correspond to 2 to 4 layers (Figure 3 H,I; Supporting Information, Figure S2 M–P, S3 B).[2d,5b] Few thick flakes of heights more than 10 nm were also observed (Figure S3 C). It is important to note that the presence of peptide nanotubes is crucial for the stability of exfoliated MoS_2, and dilution results in rapid aggregation as flocculation is observed within 15 min. Also, aggregation phenomenon during deposition/drying in solvent exfoliated MoS_2 has been previously observed.[5b] Removal of nanotubes through dilutions resulted in aggregation, as indicated from the few thick flakes. Despite the likelihood of aggregation, the presence of large numbers of thin layers indicates the efficient exfoliation by the nanotubes. Lateral lengths were found to be in the range from 78 nm to 1175 nm with a mean $\langle L \rangle = 374$ nm (Figure S3 C).

To explain the efficient exfoliation and interactions involved between MoS_2 and the peptide nanostructures, the role of the exposed surface was investigated. The solvent-exposed cationic lysine residue of Ac-KLVFFAL-NH_2 was mutated to histidine to form Ac-HLVFFAL-NH_2, which also assembled to form homogenous nanotubes of 35–40 nm (Figure 1 F). According to pK_a and hydropathy indices of the residues,[12] lysine-exposed tubes should have higher cationic charge density than the histidines. Indeed, for histidine-exposed tubes (Ac-HLVFFAL-NH_2), the dispersed amount of MoS_2 was found to be 0.14 mg mL^{-1}, which was significantly less than the Ac-KLVFFAL-NH_2 nanotubes but was still higher than the Ac-KLVFFAE-NH_2 fibers. Expectedly, as the pH increased to 9, the histidine tubes were incapable of exfoliating MoS_2 owing to the loss of cationic surface. In addition to the charge, the colloidal stability of peptide nanotubes is expected to play a crucial role in the exfoliation. To investigate this, sodium sulfate was used to counterbalance the electrostatic repulsion of Ac-KLVFFAL-NH_2 nanotubes,[13] as divalent sulfate ions are known to precipitate proteins and bundle amyloid nanotubes.[8a] Indeed, TEM confirmed bundling (Figure 2 C) with addition of SO_4^{2-} ions, and the bundled tubes were unable to exfoliate MoS_2 (Figure 2 A; Supporting Information). The amino acid L-lysine was also unable to exfoliate MoS_2, which confirmed the importance of the nanotube morphology (Figure 2 A).

To further investigate the nature of interaction between the nanotubes and the sheets, thermogravimetric analysis (TGA) was performed on the MoS_2 film obtained after filtration and washing (Supporting Information).[5a] TGA showed the MoS_2 residue was devoid of any bound peptides (Figure S9), and thus indicated the absence of any covalent interactions with the MoS_2 sheets. In this context, owing to the antiparallel out-of-register arrangement of β-amyloid ^{17}LVFFA^{21} sequences,[8a,b,9a,c] leucine residues generate hydrophobic regions on the nanotube surface, which presumably interact with the MoS_2 nanosheets through weak physical adsorption. The dual presence of hydrophobic regions and charged lysine residues on the amyloid surface has been shown to bind hydrophobic moieties of small molecules, hydrophobic 2D graphene sheets,[8b,c] and also hydrophobic patches of cationic proteins.[8a] In the present case, when strong forces are applied from tip sonication in presence of nanotubes, the van der Waals interactions between the layers of 2D nanosheets weaken[2d] and the nanotubes interact with the sheets through hydrophobic interactions. AFM showed some MoS_2 sheets where nanotubular interaction could be observed (Figure S10). The charged lysines concurrently impart colloidal stability to the exfoliated sheets, which are also prevented from reaggregation owing to the presence of charged nanotubes in the surrounding solvent environment. Thus, for exfoliation it is important to have the self-assembled nanotube surface, which is lacking in the unassembled sequences. To check this, exfoliation was attempted in presence of HFIP pretreated disassembled Ac-KLVFFA**L**-NH_2 peptides (Supporting Information). Disassembled peptides (Figure S11) were unable to exfoliate MoS_2, thus indicating the importance of the nanotube surface to interact and exfoliate MoS_2 (Figure S12).

Clearly, the extent of MoS_2 exfoliation significantly depends on the surface properties of amyloid nanostructures, such as morphology, nature of exposed surface and colloidal stabilization through electrostatic repulsion. Intriguingly, these features of amyloid nanostructures are acutely respon-

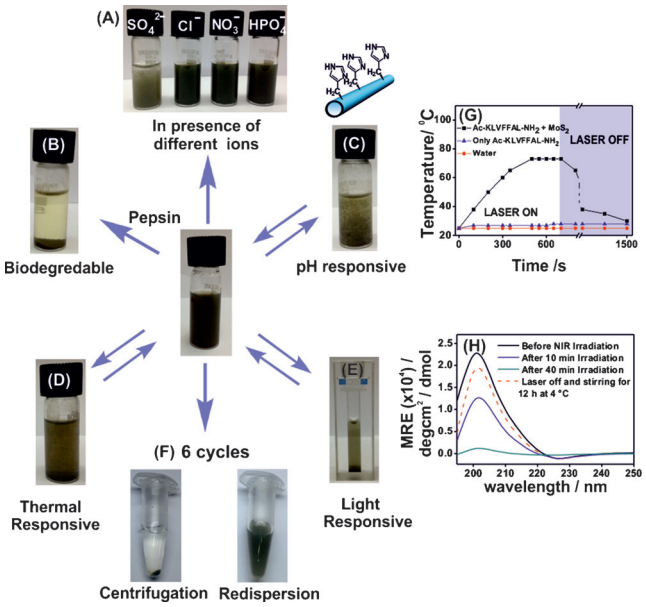

Figure 4. Responsiveness of MoS_2-amyloid peptide nanocomposites in the presence of different ions (A), biodegradability in presence of pepsin (B), pH (C), temperature (D), and light (E). F) Multiple centrifugation and redispersions cycles do not result in loss of dispersions. G) Change of temperature with time when MoS_2-amyloid peptide nanocomposites, control peptide, and only water was irradiated with a NIR laser (804 nm). H) CD spectra of MoS_2-Ac-KLVFFAL-NH_2 solutions before and after irradiation of NIR laser (804 nm).

sive towards subtle changes of the environmental inputs. We thought this responsive behavior which stems from the reversible assembly/disassembly of amyloid nanostructures can be utilized to modulate the dispersion (Figure 4). We started by changing the temperature of MoS_2-Ac-KLVFFAL-NH_2 dispersions from 25 to 65 °C and further incubation for 60 min at 65 °C, which resulted in destabilization and flocculation (Figure 4D). Interestingly, when the same destabilized dispersion was stirred for 24 h at 4 °C, a homogenous greenish black dispersion of MoS_2 was retrieved. In this regard, MoS_2 has strong near infrared (NIR) absorbance, which can be used to photothermally heat the surrounding environment. Therefore, we used a NIR laser of wavelength 804 nm with power density of 1.5 Watt cm^{-2} to irradiate an aqueous dispersion of MoS_2-Ac-KLVFFAL-NH_2 (Supporting Information). The temperature increased rapidly and resulted in boiling after irradiation for approximately 600 s (Figure 4G). The temperature decreased to room temperature within 10 min of turning off the laser. The secondary structures of cross-β-amyloid nanotubes after NIR laser irradiation were monitored by CD spectroscopy (Figure 4H).[8b,9c] Indeed, NIR irradiation resulted in a substantial decrease of the characteristic β-sheet signature, which eventually showed complete melting of the nanotubes after 40 min (Figure 4H). Flocculation could be seen in the quartz cell after 60 minutes of irradiation (Figure 4E). The dispersion was retrieved after 12 h of stirring at 4 °C, with CD showing a strong β-sheet signature (Figure 4H), indicating the reassembly of the nanostructures. To demonstrate pH responsiveness, exfoliated MoS_2 in Ac-HLVFFAL-NH_2 nanotubes was used. The dispersions responded to subtle changes in pH from 6.0 (redispersed in water) to 8, as flocculation and precipitation was observed (Figure 4C; Supporting Information, Figure S13). The dispersion was completely recoverable when the pH was adjusted back to 4.5 through addition of trifluoroacetic acid. This unique environmental input-dependent exfoliation of MoS_2 can have applications in diverse fields. The dimension of the amyloid nanotubes also allows easy separation from the medium. This attribute was exploited to isolate the exfoliated MoS_2 from aqueous dispersions through centrifugation at 17000 rpm. This resulted in complete separation of the MoS_2-peptide composites as a black pellet (Figure 4F) and colorless supernatant. Removal of supernatant and addition of fresh aqueous solution and subsequent stirring for 30 min resulted in retrieval of the dispersed MoS_2, as evident from the UV/Vis spectra (Figure S14). Intriguingly, this process of centrifugation and redispersion could be done for at least six consecutive times, and thus may have potential applications in catalysis. The biodegradability of the dispersion was checked by addition of pepsin, a protease enzyme that resulted in flocculation after 2 days (Figure 4B). This happened due to digestion of Ac-KLVFFAL-NH_2, which concomitantly results in loss of dispersion (Figure 4B; Supporting Information, Figures S15–S18). The responsiveness of the dispersions, specifically towards divalent ions like SO_4^{2-}, was also evident, as addition of different monovalent anions did not result in loss of dispersions (Figure 4A). Although the amyloid nanostructures used thus far were homogenous, to find the effect of polymorphism on stimuli-responsiveness, the temperature-responsiveness of 1:1 mixture of Ac-KLVFFAE-NH_2 fibers and Ac-KLVFFAL-NH_2 nanotubes was tested. Upon heat treatment, the incubation time required to destabilize the dispersion increased from 60 to 95 min, indicating the importance of homogeneity for responsiveness. Finally, the concentration of dispersed MoS_2 could be increased by varying the sonication time (Figure S18).[5a]

In summary, we have found a unique and environmentally benign way of exfoliating MoS_2 in aqueous milieu. The simple procedure of creating MoS_2 aqueous dispersion, the design flexibility of the exfoliating agents, and the stimuli-responsiveness of the dispersions make developed MoS_2-peptide nanohybrids applicable in diverse fields.

Acknowledgements

D.D. and N.K. are thankful to DST, India for financial assistance through INSPIRE Grant (No. IFA12-CH-64). Authors gratefully acknowledge Dr. S. Mukhopadhyay and P. Dogra, IISER Mohali, for their help, and Dr. Mahesh Kumar, NPL Delhi, for NIR laser.

Keywords: 2D materials · amyloid nanostructures · liquid exfoliation · molybdenum · supramolecular chemistry

How to cite: *Angew. Chem. Int. Ed.* **2016**, *55*, 7772–7776
Angew. Chem. **2016**, *128*, 7903–7907

[1] a) H. Li, J. Wu, Z. Yin, H. Zhang, *Acc. Chem. Res.* **2014**, *47*, 1067–1075; b) C. N. R. Rao, H. S. S. Ramakrishna Matte, U.

Maitra, *Angew. Chem. Int. Ed.* **2013**, *52*, 13162 – 13185; *Angew. Chem.* **2013**, *125*, 13400 – 13424; c) C. Tan, H. Zhang, *Chem. Soc. Rev.* **2015**, *44*, 2713 – 2731; d) V. Nicolosi, M. Chhowalla, M. G. Kanatzidis, M. S. Strano, J. N. Coleman, *Science* **2013**, *340*, 1226419; e) P. Laaksonen, M. Kainlauri, T. Laaksonen, A. Shchepetov, H. Jiang, J. Ahopelto, M. B. Linder, *Angew. Chem. Int. Ed.* **2010**, *49*, 4946 – 4949; *Angew. Chem.* **2010**, *122*, 5066 – 5069; f) S. N. Kim, Z. Kuang, J. M. Slocik, S. E. Jones, Y. Cui, B. L. Farmer, M. C. McAlpine, R. R. Naik, *J. Am. Chem. Soc.* **2011**, *133*, 14480 – 14483; g) Y. Cui, S. N. Kim, R. R. Naik, M. C. McAlpine, *Acc. Chem. Res.* **2012**, *45*, 696 – 704; h) S. Park, R. S. Ruoff, *Nat. Nanotechnol.* **2009**, *4*, 217 – 224; i) X. Huang, Z. Y. Yin, S. X. Wu, X. Y. Qi, Q. Y. He, Q. C. Zhang, Q. Y. Yan, F. Boey, H. Zhang, *Small* **2011**, *7*, 1876 – 1902; j) X. Huang, X. Y. Qi, F. Boey, H. Zhang, *Chem. Soc. Rev.* **2012**, *41*, 666 – 686; k) H. Zhang, *ACS Nano* **2015**, *9*, 9451 – 9469; l) X. Huang, C. L. Tan, Z. Y. Yin, H. Zhang, *Adv. Mater.* **2014**, *26*, 2185 – 2204; m) X. Huang, Z. Y. Zeng, H. Zhang, *Chem. Soc. Rev.* **2013**, *42*, 1934 – 1946; n) C. L. Tan, H. Zhang, *J. Am. Chem. Soc.* **2015**, *137*, 12162 – 12174.

[2] a) C. N. R. Rao, K. Gopalakrishnan, U. Maitra, *ACS Appl. Mater. Interfaces* **2015**, *7*, 7809 – 7832; b) U. Halim, C. R. Zheng, Y. Chen, Z. Lin, S. Jiang, R. Cheng, Y. Huang, X. Duan, *Nat. Commun.* **2013**, *4*, 2213; c) S. S. Chou, M. De, J. Kim, S. Byun, C. Dykstra, J. Yu, J. Huang, V. P. Dravid, *J. Am. Chem. Soc.* **2013**, *135*, 4584 – 4587; d) Z. Y. Zeng, Z. Y. Yin, X. Huang, H. Li, Q. Y. He, G. Lu, F. Boey, H. Zhang, *Angew. Chem. Int. Ed.* **2011**, *50*, 11093 – 11097; *Angew. Chem.* **2011**, *123*, 11289 – 11293.

[3] a) Y. Sun, S. Gao, F. Lei, Y. Xie, *Chem. Soc. Rev.* **2015**, *44*, 623 – 636; b) J. M. Yun, Y. J. Noh, C. H. Lee, S. I. Na, S. Lee, S. M. Jo, H. I. Joh, D. Y. Kim, *Small* **2014**, *10*, 2319 – 2324; c) Y. Chen, C. Tan, H. Zhang, L. Wang, *Chem. Soc. Rev.* **2015**, *44*, 2681 – 2701; d) X. Huang, Z. Y. Zeng, S. Y. Bao, M. F. Wang, X. Y. Qi, Z. X. Fan, H. Zhang, *Nat. Commun.* **2013**, *4*, 1444; e) Z. Y. Zeng, C. L. Tan, X. Huang, S. Y. Bao, H. Zhang, *Energy Environ. Sci.* **2014**, *7*, 797 – 803; f) W. J. Zhou, Z. Y. Yin, Y. P. Du, X. Huang, Z. Y. Zeng, Z. X. Fan, H. Liu, J. Y. Wang, H. Zhang, *Small* **2013**, *9*, 140 – 147; g) X. Gu, W. Cui, H. Li, Z. W. Wu, Z. Y. Zeng, S. T. Lee, H. Zhang, B. Q. Sun, *Adv. Energy Mater.* **2013**, *3*, 1262 – 1268; h) D. Voiry, A. Goswami, R. Kappera, C. D. C. C. E. Silva, D. Kaplan, T. Fujita, M. Chen, T. Asefa, M. Chhowalla, *Nat. Chem.* **2015**, *7*, 45 – 49; i) M. Chhowalla, H. S. Shin, G. Eda, L. J. Li, K. Loh, H. Zhang, *Nat. Chem.* **2013**, *5*, 263 – 275; j) Y. Guo, K. Xu, C. Wu, J. Zhao, Y. Xie, *Chem. Soc. Rev.* **2015**, *44*, 637 – 646; k) M. Chhowalla, Z. F. Liu, H. Zhang, *Chem. Soc. Rev.* **2015**, *44*, 2584 – 2586.

[4] a) W. Yin, L. Yan, J. Yu, G. Tian, L. Zhou, X. Zheng, X. Zhang, Y. Yong, J. Li, Z. Gu, Y. Zhao, *ACS Nano* **2014**, *8*, 6922 – 6933; b) T. Liu, C. Wang, X. Gu, H. Gong, L. Cheng, X. Shi, L. Feng, B. Sun, Z. Liu, *Adv. Mater.* **2014**, *26*, 3433 – 3440; c) T. Liu, C. Wang, W. Cui, H. Gong, C. Liang, X. Shi, Z. Li, B. Sun, Z. Liu, *Nanoscale* **2014**, *6*, 11219 – 11225; d) W. Zhang, Y. Wang, D. Zhang, S. Yu, W. Zhu, J. Wang, F. Zheng, S. Wang, J. Wang, *Nanoscale* **2015**, *7*, 10210 – 10217; e) S. S. Chou, B. Kaehr, J. Kim, B. M. Foley, M. De, P. E. Hopkins, J. Huang, C. J. Brinker, V. P. Dravid, *Angew. Chem. Int. Ed.* **2013**, *52*, 4160 – 4164; *Angew. Chem.* **2013**, *125*, 4254 – 4258.

[5] a) R. J. Smith, P. J. King, M. Lotya, C. Wirtz, U. Khan, S. De, A. O'Neill, G. S. Duesberg, J. C. Grunlan, G. Moriarty, J. Chen, J. Wang, A. I. Minett, V. Nicolosi, J. N. Coleman, *Adv. Mater.* **2011**, *23*, 3944 – 3948; b) J. N. Coleman, M. Lotya, A. O'Neill, S. D. Bergin, P. J. King, U. Khan, K. Young, A. Gaucher, S. De, R. J. Smith, I. V. Shvets, S. K. Arora, G. Stanton, H. Y. Kim, K. Lee, G. T. Kim, G. S. Duesberg, T. Hallam, J. J. Boland, J. J. Wang, J. F. Donegan, J. C. Grunlan, G. Moriarty, A. Shmeliov, R. J. Nicholls, J. M. Perkins, E. M. Grieveson, K. Theuwissen, D. W. McComb, P. D. Nellist, V. Nicolosi, *Science* **2011**, *331*, 568 – 571.

[6] L. Dong, S. Lin, L. Yang, J. Zhang, C. Yang, D. Yang, H. Lu, *Chem. Commun.* **2014**, *50*, 15936 – 15939.

[7] a) R. Bissessur, J. L. Schindler, C. R. Kannewurf, M. Kanatzidis, *Mol. Cryst. Liq. Cryst.* **1994**, *245*, 249 – 254; b) L. Wang, J. Schindler, J. A. Thomas, C. R. Kannewurf, M. G. Kanatzidis, *Chem. Mater.* **1995**, *7*, 1753 – 1755.

[8] a) N. Kapil, A. Singh, D. Das, *Angew. Chem. Int. Ed.* **2015**, *54*, 6492 – 6495; *Angew. Chem.* **2015**, *127*, 6592 – 6595; b) W. S. Childers, A. K. Mehta, K. Lu, D. G. Lynn, *J. Am. Chem. Soc.* **2009**, *131*, 10165 – 10172; c) C. Li, J. Adamcik, R. Mezzenga, *Nat. Nanotechnol.* **2012**, *7*, 421 – 427; d) C. Li, R. Mezzenga, *Nanoscale* **2013**, *5*, 6207 – 6218; e) S. Li, A. N. Sidorov, A. K. Mehta, A. J. Bisignano, D. Das, W. S. Childers, E. Schuler, Z. Jiang, T. M. Orlando, K. Berland, D. G. Lynn, *Biochemistry* **2014**, *53*, 4225 – 4227; f) S. Bolisetty, J. Adamcik, J. Heier, R. Mezzenga, *Adv. Funct. Mater.* **2012**, *22*, 3424 – 3428; g) I. Cherny, E. Gazit, *Angew. Chem. Int. Ed.* **2008**, *47*, 4062 – 4069; *Angew. Chem.* **2008**, *120*, 4128 – 4136; h) Q. Li, L. Liu, S. Zhang, M. Xu, X. Wang, C. Wang, F. Besenbacher, M. Dong, *Chem. Eur. J.* **2014**, *20*, 7236 – 7240; i) J. Li, Q. Han, X. Wang, N. Yu, L. Yang, R. Yang, C. Wang, *Small* **2014**, *10*, 4386 – 4394; j) C. Meier, I. Lifincev, M. E. Welland, *Biomacromolecules* **2015**, *16*, 558 – 563; k) P. Laaksonen, A. Walther, J. M. Malho, M. Kainlauri, O. Ikkala, M. B. Linder, *Angew. Chem. Int. Ed.* **2011**, *50*, 8688 – 8691; *Angew. Chem.* **2011**, *123*, 8847 – 8850; l) B. G. Cousins, A. K. Das, R. Sharma, Y. Li, J. P. McNamara, I. H. Hillier, I. A. Kinloch, R. V. Ulijn, *Small* **2009**, *5*, 587 – 590; m) S. K. Samanta, A. Pal, S. Bhattacharya, C. N. R. Rao, *J. Mater. Chem.* **2010**, *20*, 6881 – 6890; n) Y. Li, B. G. Cousins, R. V. Ulijn, I. A. Kinloch, *Langmuir* **2009**, *25*, 11760 – 11767; o) A. Pal, B. S. Chhikara, A. Govindaraj, S. Bhattacharya, C. N. R. Rao, *J. Mater. Chem.* **2008**, *18*, 2593 – 2600.

[9] a) C. Liang, R. Ni, J. E. Smith, W. S. Childers, A. K. Mehta, D. G. Lynn, *J. Am. Chem. Soc.* **2014**, *136*, 15146 – 15149; b) J. Nanda, A. Biswas, B. Adhikari, A. Banerjee, *Angew. Chem. Int. Ed.* **2013**, *52*, 5041 – 5045; *Angew. Chem.* **2013**, *125*, 5145 – 5149; c) A. K. Mehta, K. Lu, W. S. Childers, Y. Liang, S. N. Dublin, J. Dong, J. P. Snyder, S. V. Pingali, P. Thiyagarajan, D. G. Lynn, *J. Am. Chem. Soc.* **2008**, *130*, 9829 – 9835; d) A. Shome, S. Debnath, P. K. Das, *Langmuir* **2008**, *24*, 4280 – 4288; e) S. Basak, J. Nanda, A. Banerjee, *Chem. Commun.* **2014**, *50*, 2356 – 2359; f) T. Kar, S. Debnath, D. Das, A. Shome, P. K. Das, *Langmuir* **2009**, *25*, 8639 – 8648; g) D. Das, S. Roy, S. Debnath, P. K. Das, *Chem. Eur. J.* **2010**, *16*, 4911 – 4922; h) T. P. Knowles, A. W. Fitzpatrick, S. Meehan, H. R. Mott, M. Vendruscolo, C. M. Dobson, M. E. Welland, *Science* **2007**, *318*, 1900 – 1903; i) T. P. J. Knowles, M. J. Buehler, *Nat. Nanotechnol.* **2011**, *6*, 469 – 479; j) R. Paparcone, S. W. Cranford, M. J. Buehler, *Nanoscale* **2011**, *3*, 1748 – 1755.

[10] C. Backes, R. J. Smith, N. McEvoy, N. C. Berner, D. McCloskey, H. C. Nerl, A. O'Neill, P. J. King, T. Higgins, D. Hanlon, N. Scheuschner, J. Maultzsch, L. Houben, G. S. Duesberg, J. F. Donegan, V. Nicolosi, J. N. Coleman, *Nat. Commun.* **2014**, *5*, 4576.

[11] a) S. Jiménez Sandoval, D. Yang, R. F. Frindt, J. C. Irwin, *Phys. Rev. B* **1991**, *44*, 3955 – 3962; b) G. L. Frey, K. J. Reynolds, R. H. Friend, H. Cohen, Y. Feldman, *J. Am. Chem. Soc.* **2003**, *125*, 5998 – 6007.

[12] J. Kyte, R. F. Doolittle, *J. Mol. Biol.* **1982**, *157*, 105 – 132.

[13] K. Lu, L. Guo, A. K. Mehta, W. S. Childers, S. N. Dublin, S. Skanthakumar, V. P. Conticello, P. Thiyagarajan, R. P. Apkarian, D. G. Lynn, *Chem. Commun.* **2007**, 2729 – 2731.

Received: October 25, 2015
Revised: January 3, 2016
Published online: February 16, 2016

